

An *rhs* gene of *Pseudomonas aeruginosa* encodes a virulence protein that activates the inflammasome

Vanderlene L. Kung^a, Sonal Khare^b, Christian Stehlik^b, Elizabeth M. Bacon^a, Ami J. Hughes^a, and Alan R. Hauser^{a,b,1}

^aDepartment of Microbiology-Immunology and ^bDepartment of Medicine, Northwestern University Feinberg School of Medicine, Chicago, IL 60611

Edited by John J. Mekalanos, Harvard Medical School, Boston, MA, and approved December 15, 2011 (received for review June 9, 2011)

The *rhs* genes are a family of enigmatic composite genes, widespread among Gram-negative bacteria. In this study, we characterized *rhsT*, a *Pseudomonas aeruginosa* *rhs* gene that encodes a toxic protein. Expression of *rhsT* was induced upon contact with phagocytic cells. The RhsT protein was exposed on the bacterial surface and translocated into phagocytic cells; these cells subsequently underwent inflammasome-mediated death. Moreover, RhsT enhanced host secretion of the potent proinflammatory cytokines IL-1 β and IL-18 in an inflammasome-dependent manner. In a mouse model of acute pneumonia, infection with a *P. aeruginosa* strain lacking *rhsT* was associated with less IL-18 production, fewer recruited leukocytes, reduced pulmonary bacterial load, and enhanced animal survival. Thus, *rhsT* encodes a virulence determinant that activates the inflammasome.

rhs element | YD repeat | pathogenesis

The *rhs* genes are a widely distributed, enigmatic family of horizontally acquired genes. First described in *Escherichia coli* in the 1980s (1), *rhs* genes have subsequently been found in a broad range of Gram-negative bacteria, including other members of the *Enterobacteriaceae*, such as *Salmonella*, *Yersinia*, and *Photobacterium*, as well as the *Pseudomonadaceae*, *Flavobacteriaceae*, *Neisseriaceae*, *Myxococcaceae*, and *Vibrionaceae*. An observed chromosomal rearrangement following recombination between distinct *rhs* genes in *E. coli* led to the name “rearrangement hot spot (*rhs*)” (1). However, recombination events are no longer thought to be a biologically relevant aspect of *rhs* genes (2). Despite their ubiquity and the many years since their discovery, *rhs* genes have not been assigned a definitive function, and even clear evidence of gene expression has been elusive (3).

Interest in *rhs* genes has been fueled by their unique structure. These genes, which generally range from 2 to 12 kb in size, exhibit a bipartite structure consisting of two distinct sequences: a long core followed by a short tip (Fig. S1A). Core sequences are GC-rich and display a high degree of intra- and interspecies sequence conservation. In contrast, tip sequences are relatively GC-poor and are highly variable even between closely related *rhs* genes. Corresponding to the *rhs* gene core and tip sequences, the proteins predicted to be encoded by *rhs* genes also contain two regions: a large core domain and a short C-terminal tip domain. Rhs core domains are defined by a variable number of tyrosine-aspartate (YD) repeats and are separated from their cognate tip domains by a 61-amino acid hyperconserved region ending in the consensus sequence PXXXXDPXGL (2). Some predicted Rhs proteins also contain a large N-terminal domain. Putative Rhs proteins are predicted to be hydrophilic, and the products of some *rhs* genes have features of bacteriocins or capsule transport proteins (4–6). Furthermore, Rhs protein YD-repeats and hyperconserved regions display sequence similarity with toxins produced by bacteria that infect insects (7). These observations suggest that some *rhs* genes encode surface exposed or secreted proteins.

rhsT is an *rhs* gene found within the genomic island PAGI-9 of *Pseudomonas aeruginosa* (Fig. S1A). This gene was first identified in a screen for genetic elements present in the highly virulent *P. aeruginosa* strain PSE9 but absent in the relatively avirulent

strain PAO1 (8). For this reason, we examined whether *rhsT* contributed to the highly virulent phenotype of PSE9.

Results

Levels of *rhsT* mRNA Are Growth Phase-Dependent and Increase in the Context of Infection. In previous studies with bacteria grown in routine laboratory media, demonstration of *rhs* gene expression has been difficult (3). To examine the expression of *rhsT*, we performed quantitative RT-PCR analysis on bacteria grown under a variety of conditions. *rhsT* transcripts were detected in PSE9 grown in either rich (Luria-Bertani, LB) or minimal (Vogel-Bonner minimal) medium, with a trend toward higher mRNA levels in stationary phase compared with exponential phase (Fig. S1B). Interestingly, *rhsT* transcripts were increased over 30-fold (compared with exponential phase LB cultures) during growth in the presence of THP-1 cells, a human monocytic cell line. Growth of PSE9 bacteria in THP-1-conditioned medium alone (RPMI taken from THP-1 cells following 16 h of growth) did not promote *rhsT* transcription beyond that observed with laboratory media, suggesting that *rhsT* expression is induced during bacterial infection of human cultured phagocytic cells.

***rhsT* Is a 6672-bp ORF with σ^{54} –12/–24 Sequences.** To better characterize the *rhsT* gene and its regulation, we determined its transcriptional start site by 5' RACE. We obtained the 5' sequence of the *rhsT* transcript (Fig. S1A) and experimentally validated the *rhsT* transcriptional start site predicted by bioinformatic approaches. This start site was located 38-bp upstream of a predicted RhsT start codon. Inspection of sequences upstream of the *rhsT* transcriptional start site revealed consensus –12 and –24 sequences recognized by the alternative σ factor σ^{54} , which regulates diverse processes ranging from metabolism to virulence (9, 10). In addition to suggesting σ^{54} regulation, mapping of the *rhsT* transcriptional start site defined the length of the *rhsT* ORF. Two different *rhsT* translational start sites were predicted by bioinformatic approaches. EasyGene 1.2 and GeneMark.hmm for Prokaryotes 2.8 predicted a 6,672-bp ORF, and National Center for Biotechnology Information ORF Finder predicted a 6,837-bp ORF. Our 5' RACE results exclude the possibility of a 6,837-bp ORF because the beginning of the ORF precedes the *rhsT* transcriptional start site.

RhsT Is on the Bacterial Cell Surface. To further characterize the protein encoded by the *rhsT* gene, we generated an isogenic mutant (PSE9 Δ *rhsT*) in which the majority of the *rhsT* ORF is replaced by a gentamicin-resistance cassette. Furthermore, an inducible overexpression strain PSE9 Δ *rhsT*(pRHST) was generated by cloning *rhsT* into a P_{BAD}-based arabinose inducible

Author contributions: V.L.K. and A.R.H. designed research; V.L.K., S.K., E.M.B., and A.J.H. performed research; C.S. contributed new reagents/analytic tools; V.L.K. and E.M.B. analyzed data; and V.L.K. and A.R.H. wrote the paper.

The authors declare no conflict of interest.

This article is a PNAS Direct Submission.

¹To whom correspondence should be addressed. E-mail: ahauser@northwestern.edu.

This article contains supporting information online at www.pnas.org/lookup/suppl/doi:10.1073/pnas.1109285109/-DCSupplemental.

expression plasmid. Growth curves at 37 °C with shaking indicated no difference in growth rate between the parental, mutant, and overexpression strains. Immunoblot analysis using an antibody generated against a predicted peptide of RhsT was performed to determine if RhsT protein was produced in *P. aeruginosa*. Although no protein was detected in PSE9 lysates, a faint band was observed between the 238- and 268-kDa molecular weight markers in the cell lysate of PSE9 Δ *rhtS*(pRHST) induced with arabinose (Fig. 1A). This band is consistent with the predicted molecular weight of full-length RhsT (240 kDa), and was identified as RhsT by tandem mass spectrometry. Because *rhtS* genes have been predicted to encode bacterial cell surface-associated and -secreted proteins (3), we next determined whether RhsT could be detected in culture supernatant and on the bacterial cell surface. A 240-kDa band was detected in concentrated PSE9 Δ *rhtS*(pRHST) culture supernatant (Fig. 1A), and examination of fixed but nonpermeabilized PSE9 Δ *rhtS*(pRHST) bacteria grown under inducing conditions by indirect immunofluorescence revealed staining around the bacterial cell circumference (Fig. 1B). Because these bacteria were not permeabilized (Fig. S2A), this staining pattern indicated that RhsT was on the bacterial cell surface, either as a surface protein or in the process of being secreted.

RhsT Is Translocated into Eukaryotic Cells. Given that the YD-repeats and the hyperconserved region within the RhsT core domain are similar in sequence to the *Photobacterium* TccC insecticidal toxin (7), we hypothesized that RhsT is a secreted protein that is translocated into eukaryotic cells. To determine if this is indeed the case, we used the CCF2 reporter system, which is highly sensitive because it is based on enzymatic signal amplification (11). In this approach, eukaryotic cells are loaded with the fluorogenic substrate CCF2, which consists of a β -lactam ring

modified with two fluorophores that upon excitation undergo FRET to fluoresce green. In the presence of β -lactamase activity, however, the β -lactam ring is cleaved, FRET is lost, and the substrate fluoresces blue upon excitation. Thus, cells intoxicated with β -lactamase will exhibit blue fluorescence but those not intoxicated will fluoresce green. We generated a strain of PSE9 that expressed RhsT fused at its C terminus to β -lactamase (designated PSE9*rhtS*-*bla*) and used it to determine whether the RhsT protein could target the fused β -lactamase domain to the cytosol of CCF2-treated J774 cells (a macrophage-like cell line). RhsT- β -lactamase translocation into J774 cells was detected by fluorescence microscopy, which showed blue fluorescent J774 cells (Fig. S2B). These qualitative results were confirmed and quantified using blue and green fluorescence intensity measurements. As expected, cells infected with PSE9 producing RhsT- β -lactamase exhibited a relatively high blue-to-green fluorescence ratio (Fig. 2A). In contrast, low blue-to-green ratios were observed with cells infected with PSE9 producing RhsT lacking the β -lactamase domain, as well as cells infected with the control strain PSE9*gst*-*bla*, which expresses the cytoplasmic protein GST fused to β -lactamase. Thus, the elevated blue-to-green fluorescence ratio observed with PSE9*rhtS*-*bla* infection was not because of β -lactamase release following lysis of bacteria internalized by J774 cells. Consistent with this observation, RhsT translocation was not abrogated in J774 cells pretreated with cytochalasin D, an inhibitor of phagocytosis, indicating that bacterial internalization was not necessary for RhsT translocation (Fig. 2A). Interestingly, cytochalasin D treatment did eliminate the background blue fluorescence observed with the PSE9 and PSE9*gst*-*bla* controls, suggesting that phagocytosis followed by release of endogenous *P. aeruginosa* β -lactamases, such as AmpC, contributed to these background levels (12). Taken together, these results indicate that RhsT is translocated into J774 cells.

RhsT Translocation Is Associated with Death and Inflammasome Activation in Monocyte/Macrophage-Like Cells.

We next examined the fate of J774 macrophage-like cells following infection with RhsT⁺ bacteria by using lactate dehydrogenase (LDH)-release as a marker for cell death. PSE9 killed J774 cells, and disruption of *rhtS* reduced this killing by ~50% (Fig. 2B). This RhsT-dependent cytotoxicity was abrogated by pretreatment of J774 cells with the caspase-1 inhibitor YVAD, suggesting that host cell death caused by RhsT involves inflammasome signaling.

Mammalian cells detect bacterial factors within their cytosol by multiprotein complexes known as inflammasomes. Inflammasomes assemble around NOD-like receptor or HIN-200 proteins and cause the activation of caspase-1 by a process requiring the adaptor protein ASC. To further explore the relationship between host cell death caused by RhsT and inflammasome activation, we used THP-1 human monocytic-like cells, which have become a model for studying inflammasome activation. THP-1 cells with intact or disrupted inflammasomes because of a deficiency in ASC were infected with PSE9 or PSE9 Δ *rhtS*. In THP-1 cells with intact inflammasomes, PSE9 caused twice as much cell death as PSE9 Δ *rhtS* (Fig. S3A). In contrast, both strains of bacteria caused similar amounts of cell death in THP-1 cells deficient in ASC (Fig. S3A and B). Next, we determined whether RhsT by itself was sufficient to mediate host cell killing. Transfection of an *rhtS*-expressing construct indicated that RhsT was indeed sufficient to cause THP-1 cell lysis (Fig. S3C and D). Significantly less cell lysis was observed in ASC-deficient THP-1 cells transfected with *rhtS*, indicating that in the context of transfection, RhsT-mediated host cell lysis is dependent in part on the inflammasome adapter protein ASC.

Inflammasome activation is associated with activation of caspase-1, which results in the processing and subsequent release of cytokines IL-1 β and IL-18. To further evaluate whether RhsT activates host cell inflammasomes, we used ELISAs to measure

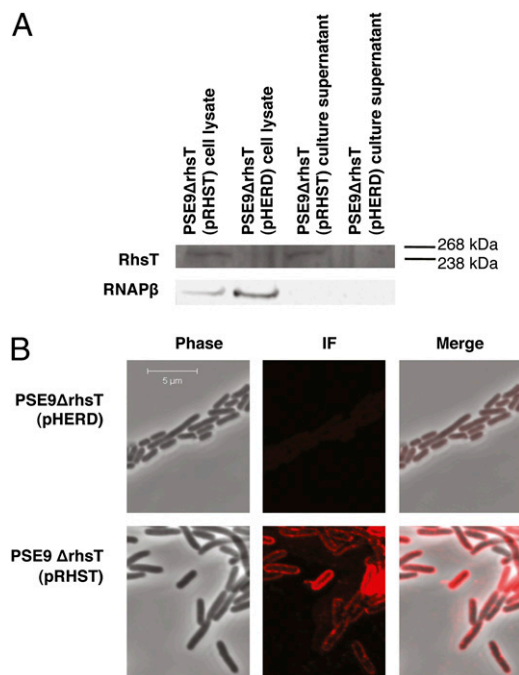


Fig. 1. Detection of RhsT by immunoblot and indirect immunofluorescence microscopy. (A) Immunoblot analysis of cell lysates and culture supernatants from PSE9 Δ *rhtS*(pRHST) and PSE9 Δ *rhtS*(pHERD) (PSE9 Δ *rhtS* containing the empty arabinose inducible vector). RNAP β was used as a loading control and a control for cell lysis in culture supernatants. (B) Visualization by indirect immunofluorescence microscopy of RhsT in PSE9 Δ *rhtS*(pHERD) and PSE9 Δ *rhtS*(pRHST) bacteria that were fixed but not permeabilized.

insertion mutagenesis screen for genes required for calf intestine colonization; however, the *rhsA* insertion mutant was not further characterized (19). An endosymbiotic bacterium carrying an *rhs* gene was associated with enhanced protection of insect hosts from parasitic wasp larvae (20), and an *rhs* gene encoded protein in *Xenorhabdus bovienii* was toxic to nematodes (GenBank accession no. CAC19493). Other members of the *rhs* gene family appear to interact with bacteria instead of eukaryotic cells. Early work by Vlazny and Hill indicated that *rhsA* of *E. coli* had features of a bacteriocin-encoding gene (21). Sisto et al. identified an *rhs* gene in *Pseudomonas savastoni* with similar properties (4). Consistent with these reports, subsequent bioinformatics analysis has linked some *rhs* genes to a large family of nucleases and nucleic acid deaminases, some of which function as bacteriocins (22). McNulty et al., however, have linked the *rhsA* gene of *E. coli* to polysaccharide transport (6), an observation supported by the similarity between the YD-repeats of putative Rhs proteins and those of teneurin-1, a eukaryotic protein that binds heparin (23). Taken together, these findings suggest that *rhs* genes encode a large family of proteins with a variety of activities and cell targets. Whether additional Rhs proteins act as virulence factors in mammals is currently being investigated.

Our results indicate that at least the C-terminal tip of RhsT is translocated into monocyte/macrophage-like cells, but it remains to be determined whether full-length RhsT is translocated into eukaryotic cells. Some large toxins, such as MARTX toxins and the large clostridial toxins, are secreted as full-length proteins that are proteolytically processed subsequent to entering host cells (24). Other large toxins, such as the contact-dependent inhibition proteins, are thought to be expressed as full-length proteins on the bacterial cell surface but function to deliver only a C-terminal domain to susceptible cells (25). We were unable to detect the RhsT protein inside eukaryotic cells by immunoblotting with antibodies to RhsT or β -lactamase, suggesting the amount of RhsT translocation is below the limit of antibody detection. The secretion mechanisms responsible for RhsT transport to the bacterial cell surface and translocation into eukaryotic cells is also unclear. As RhsT does not have an identifiable N-terminal Tat or Sec signal sequence, secretion is unlikely to proceed through the type II or type V secretion systems. Secretion may be through one of the one-step secretion systems present in *P. aeruginosa* (type I, III, or VI) or through outer membrane vesicles. Alternatively, as mentioned above, RhsT may not be secreted at all but rather be directly inserted into host cells by a mechanism similar to that described for contact-dependent inhibition proteins. In this regard, it is interesting that *rhs* genes and genes encoding toxins of contact-dependent inhibition systems have been linked by bioinformatic approaches (22).

RhsT-dependent inflammasome activation serves as further evidence of RhsT translocation into host cells. RhsT caused increased release of the cytokines IL-1 β and IL-18 in an ASC- and caspase-1-dependent manner. It is unclear whether RhsT itself directly activates inflammasome signaling by gaining access to the cytosol and interacting with a sensor protein, or if inflammasome activation is indirect, resulting from the sensing of RhsT-induced injury to the host cell. Some speculations on the mechanism of RhsT-dependent inflammasome activation can be made by comparing RhsT to other inflammasome-activating bacterial toxins. RhsT bears neither primary sequence nor secondary structure similarity to the majority of characterized inflammasome-activating bacterial toxins, which are pore-forming toxins thought to indirectly trigger inflammasome activation through K⁺ efflux (26). RhsT does, however, share some similarities with the inflammasome-activating toxins TcdA and TcdB produced by *Clostridium difficile*. Like RhsT, TcdA/B are large multidomain toxins, and the YD-repeats in the RhsT core

domain are similar in sequence to the TcdA/B C-terminal repeats thought to mediate host cell binding. A recent study found that purified TcdB protein is sufficient for inflammasome activation, and interestingly this activation is independent of TcdB enzymatic activity (27). Although it is intriguing to speculate that a common fold shared between the RhsT core domain and the TcdA/B C-terminal domain is involved in inflammasome activation, the RhsT domains necessary for inflammasome activation are not currently known.

Although the inflammasome is a component of the host innate immune system and inflammasome activation often functions to eliminate bacteria during early infection, certain microbes can co-opt the inflammasome to cause excessive inflammation. For example, *Shigella* spp. and *Salmonella enterica* secrete IpaB and SipB, respectively, to activate caspase-1 and cause IL-1 β release. The subsequent excessive inflammation that develops is thought to be a critical step in the pathogenesis of these bacteria (16, 28, 29). A similar mechanism has been proposed for the clostridial toxins TcdA/B (27). We found that RhsT⁺ *P. aeruginosa* strains were associated with robust inflammation in the lungs of infected mice. Whether enhanced inflammation led to increased bacterial numbers or vice versa cannot be directly determined from our data. However, RhsT-associated elevation of IL-18 in the lungs occurred as early as 4 h postinfection, when equivalent numbers of PSE9 and PSE9 Δ *rhsT* bacteria were present, indicating that proinflammatory cytokine levels were not solely driven by differences in bacterial numbers. Rather, excessive inflammation driven by inflammasome activation and subsequent IL-1 β and IL-18 release may have been at least partly responsible for the increased numbers of RhsT⁺ *P. aeruginosa* bacteria in the lungs. Increased levels of these cytokines have been shown to be detrimental to the clearance of *P. aeruginosa* in animal models (13, 14), and elevated IL-1 β in BAL fluid correlates with bacterial persistence in the lungs of human intensive-care unit patients (30). Thus, in our mouse model of acute *P. aeruginosa* pneumonia, RhsT-dependent enhancement of proinflammatory cytokine production and leukocyte infiltration may function as a virulence mechanism. Alternatively, RhsT may possess undefined intrinsic activity that causes tissue injury independent of inflammasome activation, and this activity may be responsible for the bacterial persistence and mortality observed in the mouse model of pneumonia. Finally, it remains possible that RhsT is acting indirectly to potentiate the activity of another *P. aeruginosa* virulence determinant. Experiments are underway to distinguish these possibilities.

In summary, the *rhsT* gene of *P. aeruginosa* encodes a unique virulence determinant that activates the inflammasome and plays an important role in the pathogenesis of pneumonia. This finding suggests that other members of the widely distributed *rhs* family of genes may also contribute to pathogenesis.

Materials and Methods

Bacterial strains, culture conditions, cell lines, 5' RACE, immunoblotting, tandem mass spectrometry, transfections, and cytokine assays are described in detail in *SI Materials and Methods* and *Tables S1–S3*.

Quantitative Real-Time PCR. PSE9 cultures were grown at 37 °C with shaking to either stationary or exponential phase. Stationary phase cultures were defined as cultures grown for 16 h, and exponential phase cultures were grown by subculturing overnight cultures in fresh medium to an OD of 0.300. For infection, bacteria were incubated with THP-1 cells for 2.5 h at a multiplicity of infection (MOI) of 20.

For all conditions, total RNA was used to generate cDNA, and quantitative RT-PCR was performed with B-R SYBR Green SuperMix for iQ (Quanta Biosciences). See *SI Materials and Methods* for more detail.

Indirect Immunofluorescence Microscopy. Bacteria were grown for 17 h in LB medium at 37 °C with shaking and then subcultured with 0.02% (wt/vol) arabinose (Sigma) for 2 h. Bacteria were then either fixed with PBS

containing 2.4% (vol/vol) formaldehyde, 0.04% (vol/vol) glutaraldehyde, or fixed and permeabilized with cold acetone. RhsT was detected with a rabbit antibody generated against an RhsT peptide (21st Century Biochemicals). RNA polymerase (RNAP β) was detected with the mouse monoclonal antibody 8RB13 (Abcam). See *SI Materials and Methods* for more detail.

Cytotoxicity Assays. Cytotoxicity was measured using the CytoTox 96 Non-radioactive Cytotoxicity Assay (Promega). Where indicated, cells were pre-treated with 100 μ M Ac-YVAD-CMK (Cayman) for 45 min before infection. For all experiments, percent cell lysis = [(LDH in sample well – LDH in background well)/(LDH in Triton X-100 treated wells – LDH in background well)] \times 100. Background was taken as uninfected cells, cells transfected with empty vector (pcDNA3.1/D/V5-His), or BAL fluid from PBS-infected mice.

Translocation Assay. J774 cells seeded in 24-well black tissue culture treated plates (Wallac, PerkinElmer) were incubated with DMSO carrier control or 5 μ g/mL cytochalasin D (Sigma) for 15 min, loaded for 1 h at room temperature and 15 min at 37 $^{\circ}$ C with 1 μ M CCF2-AM (Invitrogen), and then infected at an MOI of 20. Infections proceeded in a bottom read SpectraMax M5 fluorescence plate reader at 37 $^{\circ}$ C. Excitation was set at 410 nm; emissions at 450 nm and 520 nm were recorded. Blue-to-green fluorescence ratio = (RFU_{450nm, t = 30min} – RFU_{450nm, t = 0})/(RFU_{520nm, t = 0} – RFU_{520nm, background}), where RFU is relative fluorescence units and background fluorescence is fluorescence emission from cells that were infected but not loaded with CCF2-AM. Microscopy was performed as previously described (31). For detection of RhsT- β -lactamase translocation in vivo, mice were infected with

3.0×10^6 CFU PSE9gst-*bla* or PSE9rhsT-*bla*. At 15 h postinfection, immune cells in the airways were collected by performing BAL as previously described (17). Following quantification of Trypan blue-excluding cells using a hemocytometer, 2.0×10^5 cells were loaded with 1 μ M CCF2-AM in PBS. After a 1-h incubation at room temperature protected from light, cells were fixed and analyzed by flow cytometry using a Becton Dickinson LSRFortessa instrument.

Mouse Model of Acute Pneumonia. BALB/c mice were infected as previously described (31). BAL and lung histopathology at 26 h postinfection were performed as previously described (17). Images were captured using the TissueGnostics image acquisition software TissueFAXS. For flow cytometry analysis of immune cell recruitment to the lungs, mice were killed at the indicated time points, and immune cells in the lungs were quantified as previously described (17). See *SI Materials and Methods* for more detail.

ACKNOWLEDGMENTS. We thank Scott Battle, Maureen Diaz, and Stephanie Rangel for technical assistance, and Egon Ozer, Heather Howell, and Greg Tyson for critical reading of the manuscript. Plasmids pEX100T, pX1918G, and miniCTX1 were generous gifts from Herbert Schweizer; pHERD20T was a generous gift of Hongwei Yu; pMD2.G and psPAX2 were kindly provided by Didier Trono; and strains M90T and BS176 were gifts from Arturo Zychlinsky. This work was supported by the National Institute of Health Grants R01 AI053674, K02 AI065615, R01 AI075191, and R21 AI088286 (to A.R.H.); R01 GM071723 and R21 AI082406 (to C.S.); and F30 ES016487 (to V.L.K.). The Northwestern University Cell Imaging Facility is supported by National Cancer Institute Grant CCSG P30 CA060553 awarded to the Robert H. Lurie Comprehensive Cancer Center.

- Lin RJ, Capage M, Hill CW (1984) A repetitive DNA sequence, *rhs*, responsible for duplications within the *Escherichia coli* K-12 chromosome. *J Mol Biol* 177:1–18.
- Jackson AP, Thomas GH, Parkhill J, Thomson NR (2009) Evolutionary diversification of an ancient gene family (*rhs*) through C-terminal displacement. *BMC Genomics* 10:584.
- Hill CW, Sandt CH, Vlazny DA (1994) *Rhs* elements of *Escherichia coli*: A family of genetic composites each encoding a large mosaic protein. *Mol Microbiol* 12:865–871.
- Sisto A, et al. An *Rhs*-like genetic element is involved in bacteriocin production by *Pseudomonas savastanoi* pv. *savastanoi*. *Antonie Van Leeuwenhoek* 98:505–517.
- Roh E, Heu S, Moon E (2008) Genus-specific distribution and pathovar-specific variation of the glycinecin R gene homologs in *Xanthomonas* genomes. *J Microbiol* 46: 681–686.
- McNulty C, et al. (2006) The cell surface expression of group 2 capsular polysaccharides in *Escherichia coli*: The role of KpsD, RhsA and a multi-protein complex at the pole of the cell. *Mol Microbiol* 59:907–922.
- Waterfield NR, Bowen DJ, Fetherston JD, Perry RD, Ffrench-Constant RH (2001) The *tc* genes of *Photobacterium*: A growing family. *Trends Microbiol* 9:185–191.
- Battle SE, Rello J, Hauser AR (2009) Genomic islands of *Pseudomonas aeruginosa*. *FEMS Microbiol Lett* 290:70–78.
- Potvin E, Sanschagrin F, Levesque RC (2008) Sigma factors in *Pseudomonas aeruginosa*. *FEMS Microbiol Rev* 32:38–55.
- Bernard CS, Brunet YR, Gavioli M, Llobbers R, Cascales E (2011) Regulation of type VI secretion gene clusters by sigma54 and cognate enhancer binding proteins. *J Bacteriol* 193:2158–2167.
- Charpentier X, Oswald E (2004) Identification of the secretion and translocation domain of the enteropathogenic and enterohemorrhagic *Escherichia coli* effector Cif, using TEM-1 beta-lactamase as a new fluorescence-based reporter. *J Bacteriol* 186: 5486–5495.
- Juan C, et al. (2005) Molecular mechanisms of beta-lactam resistance mediated by AmpC hyperproduction in *Pseudomonas aeruginosa* clinical strains. *Antimicrob Agents Chemother* 49:4733–4738.
- Schultz MJ, et al. (2003) Interleukin-18 impairs the pulmonary host response to *Pseudomonas aeruginosa*. *Infect Immun* 71:1630–1634.
- Schultz MJ, et al. (2002) Role of interleukin-1 in the pulmonary immune response during *Pseudomonas aeruginosa* pneumonia. *Am J Physiol Lung Cell Mol Physiol* 282: L285–L290.
- Taxman DJ, Huang MT, Ting JP (2010) Inflammasome inhibition as a pathogenic stealth mechanism. *Cell Host Microbe* 8:7–11.
- Monack DM, et al. (2000) Salmonella exploits caspase-1 to colonize Peyer's patches in a murine typhoid model. *J Exp Med* 192:249–258.
- Diaz MH, et al. (2008) *Pseudomonas aeruginosa* induces localized immunosuppression during pneumonia. *Infect Immun* 76:4414–4421.
- Takano Y, Sakamoto O, Suga M, Muranaka H, Ando M (2002) Prognostic factors of nosocomial pneumonia in general wards: A prospective multivariate analysis in Japan. *Respir Med* 96:18–23.
- van Diemen PM, Dziva F, Stevens MP, Wallis TS (2005) Identification of enterohemorrhagic *Escherichia coli* O26:H- genes required for intestinal colonization in calves. *Infect Immun* 73:1735–1743.
- Degnan PH, Moran NA (2008) Diverse phage-encoded toxins in a protective insect endosymbiont. *Appl Environ Microbiol* 74:6782–6791.
- Vlazny DA, Hill CW (1995) A stationary-phase-dependent viability block governed by two different polypeptides from the *RhsA* genetic element of *Escherichia coli* K-12. *J Bacteriol* 177:2209–2213.
- Zhang D, Iyer LM, Aravind L (2011) A novel immunity system for bacterial nucleic acid degrading toxins and its recruitment in various eukaryotic and DNA viral systems. *Nucleic Acids Res* 39:4532–4552.
- Minet AD, Rubin BP, Tucker RP, Baumgartner S, Chiquet-Ehrismann R (1999) Ten-eurin-1, a vertebrate homologue of the *Drosophila* pair-rule gene ten-m, is a neuronal protein with a novel type of heparin-binding domain. *J Cell Sci* 112:2019–2032.
- Egerer M, Satchell KJ (2010) Inositol hexakisphosphate-induced autoprocessing of large bacterial protein toxins. *PLoS Pathog* 6:e1000942.
- Aoki SK, et al. (2010) A widespread family of polymorphic contact-dependent toxin delivery systems in bacteria. *Nature* 468:439–442.
- Hamon MA, Cossart P (2011) K+ efflux, is required for histone-H3 dephosphorylation by *Listeria LLO* and other pore forming toxins. *Infect Immun* 79:2839–2846.
- Ng J, et al. (2010) *Clostridium difficile* toxin-induced inflammation and intestinal injury are mediated by the inflammasome. *Gastroenterology* 139:542–552, 552 e541–e543.
- Hersh D, et al. (1999) The *Salmonella* invasin SipB induces macrophage apoptosis by binding to caspase-1. *Proc Natl Acad Sci USA* 96:2396–2401.
- Schroeder GN, Jann NJ, Hilbi H (2007) Intracellular type III secretion by cytoplasmic *Shigella flexneri* promotes caspase-1-dependent macrophage cell death. *Microbiology* 153:2862–2876.
- Wu CL, et al. (2003) Bronchoalveolar interleukin-1 beta: A marker of bacterial burden in mechanically ventilated patients with community-acquired pneumonia. *Crit Care Med* 31:812–817.
- Diaz MH, Hauser AR (2010) *Pseudomonas aeruginosa* cytotoxin ExoU is injected into phagocytic cells during acute pneumonia. *Infect Immun* 78:1447–1456.

Supporting Information

Kung et al. 10.1073/pnas.1109285109

SI Materials and Methods

Bacterial Strains and Culture Conditions. All strains are described in Table S1. All primer sequences and plasmids used to generate modified strains are listed in Tables S2 and S3. The authenticity of all cloning constructs generated was validated by sequencing. *Pseudomonas aeruginosa* strains were grown in Luria-Bertani (LB) medium, Vogel-Bonner minimal (VBM) medium (1), or MINS medium (2). *Shigella* strains were grown in LB medium. When appropriate, medium was supplemented with carbenicillin (100 µg/mL for liquid cultures and 300 µg/mL for agar plates) or gentamicin (100 µg/mL for both liquid cultures and agar plates).

Cell Lines. J774 cells were cultured in DMEM supplemented with 10% FBS (Invitrogen), 4.5 g/L D-glucose, 4 mM L-glutamine, and 25 mM Hepes buffer (Invitrogen). THP-1 cells were cultured in RPMI medium (Invitrogen) supplemented with 10% FBS. For all infections, cells were switched to growth in FBS-free medium 30 min before infection.

THP-1 and ASC-Deficient THP-1 Cells. Stable THP-1^{shCtrl} (THP-1) and THP-1^{shASC} (hereafter referred to as ASC⁻ THP-1) cells were generated by lentiviral transduction using pLKO.1-based vectors (ASC targeting sequence: 5'-gctcttcagtttcacacca-3') and shRNA nontargeting control (Sigma) with the envelope pMD2.G and the packaging psPAX2 plasmids (Addgene plasmids 12259 and 12260) produced in HEK293T cells followed by puromycin selection. Lack of ASC protein expression in ASC⁻ THP-1 cells was verified by immunoblot analysis (Fig. S3B).

5' RACE. Total RNA was isolated from PSE9 grown to stationary phase in VBM medium. cDNA was generated using primer GSP1 and tailed with dCTP using terminal deoxy-transferase (TdT). PCR amplification was then performed on tailed cDNA template using a poly-G primer (5' RACE Abridged Anchor Primer; Invitrogen) and primer GSP2. A 1:10 dilution of the products from this first PCR was used to perform a second PCR amplification using an adapter primer (Abridged Universal Amplification Primer; Invitrogen) and primer GSP3. The product of this second PCR was analyzed by gel electrophoresis, purified, and sequenced. Samples that were processed identically but were not treated with reverse transcriptase during the first strand cDNA synthesis reaction or were not treated with TdT produced no final 5' RACE product. Results were compared with *in silico* analysis with BProm (Softberry). Primer sequences are listed in Table S2.

Quantitative Real-Time PCR. For each condition, bacteria were treated with RNAprotect (Qiagen) and total RNA extracted using the RNeasy Mini Kit (Qiagen). One microgram of total RNA was treated with Amplification Grade DNaseI (Invitrogen) and then incubated with reverse transcriptase using the Advantage RT-for-PCR approach (Clontech). Quantitative PCR was performed on cDNA with primers amplifying *rhsT* using B-R SYBR Green SuperMix for iQ (Quanta Biosciences) on a MyiQ Real-Time PCR machine (BioRad). Primers amplifying the housekeeping gene *oprL* were used as an internal control. No amplification was observed when total RNA extracts or cDNA from PSE9Δ*rhsT* cultures was used as template. Results were analyzed using the Pfaffl method. For example, the exponential phase minimal medium culture fold-change in *rhsT* expression relative to an exponential phase LB culture = $[(E_{r_{hsT}})^{-CT_{r_{hsT}}}] / [(E_{oprL})^{-CT_{oprL}}]_{\text{exponential minimal medium culture}} / [(E_{r_{hsT}})^{-CT_{r_{hsT}}}]$

$(E_{oprL})^{-CT_{oprL}}]_{\text{exponential LB culture}}$, where E is the efficiency of PCR and CT is the cycle threshold. Primer sequences are listed in Table S2.

Immunoblotting. Bacteria were grown for 17 h in LB medium supplemented with antibiotics, when appropriate, at 37 °C with shaking, and then subcultured for 3 h with 0.02% (wt/vol) arabinose (Sigma). A total of 1 mL of culture was pelleted and lysed using ReadyPreps (Epicentre) to a final volume of 200 µL with NuPAGE Antioxidant and Sample Buffer (Invitrogen). Next, 4 mL of culture supernatant was precipitated with trichloroacetic acid and resuspended to a final volume of 200 µL with NuPAGE Antioxidant and Sample Buffer (Invitrogen). A total of 15 µL of each sample were electrophoresed through a 3–8% NuPAGE Tris-Acetate gel (Invitrogen) along with a HiMark molecular weight ladder (Invitrogen). Proteins were wet-transferred to nitrocellulose membranes. Membranes were incubated with 5% (wt/vol) nonfat milk in Tris-buffered saline containing 0.05% (vol/vol) Tween, and then incubated with either primary rabbit anti-RhsT antibody (21st Century Biochemicals) followed by secondary goat anti-rabbit HRP-tagged antibody (Jackson Immunoresearch), or primary mouse monoclonal anti-RNAPβ antibody (Abcam) followed by secondary rabbit anti-mouse HRP-tagged antibody (Abcam).

Tandem Mass Spectrometry. Bacteria were grown and gel electrophoresis was performed as described above. A SimplyBlue SafeStain (Invitrogen) gel slice corresponding to the 240-kDa band visualized by immunoblotting was trypsin-digested. Chromatographic analysis using the LTQ-FT LC/MS/MS at the Chicago Biomedical Consortium-University of Illinois at Chicago Research Resources Center Proteomics and Informatics Services Facility produced 179 total spectra and 40 unique spectra covering 30% of the full length RhsT protein.

Indirect Immunofluorescence Microscopy. Bacteria were washed with 1 mM MgCl₂ in PBS and incubated with primary antibodies at 37 °C in PBS with 2% (vol/vol) FBS. Primary antibodies were detected with Alexa Fluor 555 goat anti-rabbit or Alexa Fluor 488 goat anti-mouse secondary antibodies (Invitrogen). Stained bacteria were incubated for 30 min at room temperature on poly-L-lysine (Sigma)-coated coverslips, which were then mounted with ProLong Gold antifade reagent (Invitrogen) and imaged using a Zeiss LSM 510 confocal microscope at the Northwestern University Cell Imaging Facility.

Transfections. THP-1 cells were transfected using the Neon transfection system (Invitrogen). A total of 3×10^5 cells were transfected with 1 µg of pcDNA3.1*rhsT* or pcDNA3.1D/V5-His-TOPO (Invitrogen) DNA in 48-well tissue culture treated plates. [pcDNA3.1*rhsT* was generated by cloning *rhsT* into pcDNA3.1D/V5-His-TOPO (Invitrogen) using primers pcDNA3.1*rhsT*-F and pcDNA3.1*rhsT*-R.] LPS was extracted with Triton X-114 from all DNA preps. Immunoblots using an antibody to the V5 epitope (Invitrogen) were performed to verify equal expression of RhsT in transfected THP-1 and ASC⁻ THP-1 cells (Fig. S3D). At 24 h posttransfection, culture supernatant was removed and 300 µL of fresh serum-free RPMI was added to each well. After 5 h of incubation, supernatant was collected for ELISA and cytotoxicity analysis.

Cytokine Assays. Wild-type and ASC⁻ THP-1 cells were seeded at a density of 3×10^5 cells per well and grown for 16 h. Cells were

mock pretreated with DMSO carrier or with 100 μ M Ac-YVAD-CMK (Cayman) for 45 min, then infected with bacteria at a multiplicity of infection (MOI) of 15 for *Pseudomonas* strains and an MOI of 5 for *Shigella* strains. Culture supernatants were harvested at 4 h postinfection and cleared by centrifugation at $300 \times g$ for 5 min. IL-1 β was measured using a human IL-1 β /IL-1F2 ELISA (ELISA, R&D Systems). IL-18 was captured by coating 96-well MaxiSorp plates (Nunc) with antibody specific to the mature fragment of human IL-18 (R&D Systems) and was detected using a biotinylated antibody to human IL-18 (R&D Systems). For mouse lung cytokine assays, mouse lung homogenates were cleared by centrifugation at $300 \times g$ for 5 min before cytokine measurement using a mouse IL-18 ELISA kit (MBL).

Mouse Model of Acute Pneumonia. For survival experiments, mice were monitored for severe illness for 7 d. Severely ill mice were

killed and scored as dead. In persistence and dissemination experiments, mice were killed at the indicated time points. Lungs and spleens were then aseptically removed and homogenized in PBS. CFU in these organs were enumerated by plating homogenates on LB agar. In competition experiments, mice were concomitantly infected with an equal ratio of PSE9 and PSE9 Δ *rhsT*, which contains a gentamicin-resistance cassette. At 26 h post-infection, the ratios of PSE9 Δ *rhsT* CFU to PSE9 CFU in the lungs and spleen were quantified by plating lung and spleen homogenates onto LB plates with or without gentamicin supplementation. Competitive indices were calculated as the ratio $(PSE9\Delta rhsT \text{ CFU}/PSE9 \text{ CFU})_{\text{output}}/(PSE9\Delta rhsT \text{ CFU}/PSE9 \text{ CFU})_{\text{input}}$. All experiments were approved by the Northwestern University Animal Care and Use Committee.

1. Vogel HJ, Bonner DM (1956) Acetylornithinase of *Escherichia coli*: Partial purification and some properties. *J Biol Chem* 218:97–106.

2. Nicas TI, Iglewski BH (1984) Isolation and characterization of transposon-induced mutants of *Pseudomonas aeruginosa* deficient in production of exoenzyme S. *Infect Immun* 45:470–474.

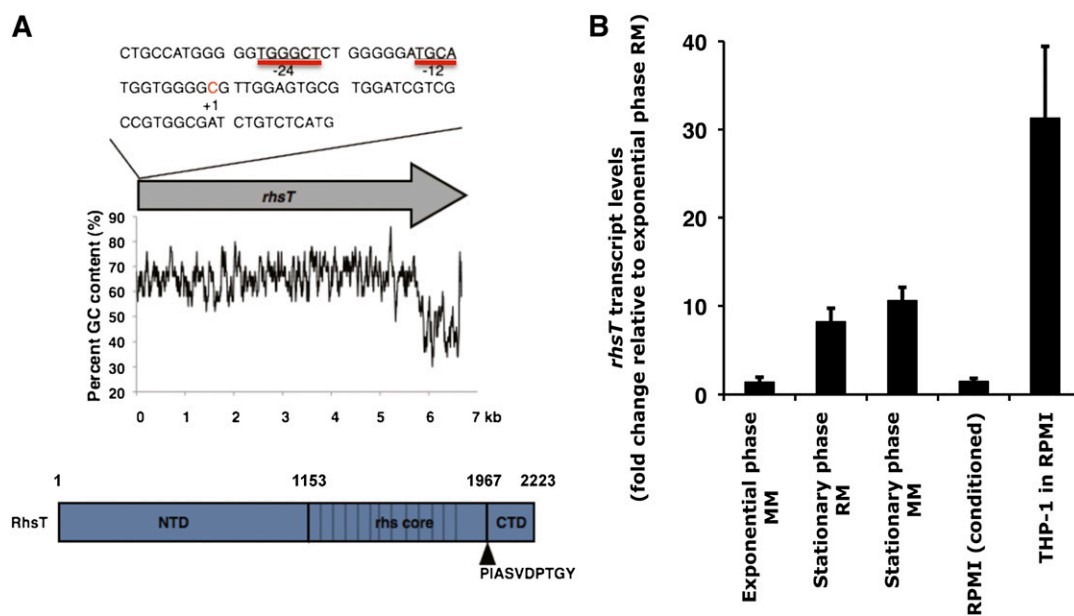


Fig. S1. Depiction of the *rhsT* gene and evaluation of *rhsT* transcript levels under different growth conditions. (A) RhsT can be divided into three domains: an N-terminal domain (NTD) with sequence similarity to the TcdA/B toxin binding/delivery proteins (1); an Rhs core domain containing 12 YD-repeats and ending in the sequence PIASVDPTGY; and a C-terminal domain (CTD) with no sequence similarity to other proteins in the database. The NTD-encoding and core sequences of *rhsT* have a 65% GC content whereas the tip sequence has a 45% GC content. The *rhsT* transcriptional start site determined by 5' RACE is indicated in red. Predicted σ^{54} -12/-24 sequences are underlined. (B) Quantitative RT-PCR analysis of *rhsT* expression normalized to that of the *oprL* reference gene presented as fold change relative to levels observed during exponential growth in rich medium. MM, minimal medium; RM, rich medium. Data are shown as means \pm SEM ($n = 3$).

1. Waterfield NR, Bowen DJ, Fetherston JD, Perry RD, Ffrench-Constant RH (2001) The *tc* genes of *Photobacterium*: A growing family. *Trends Microbiol* 9:185–191.

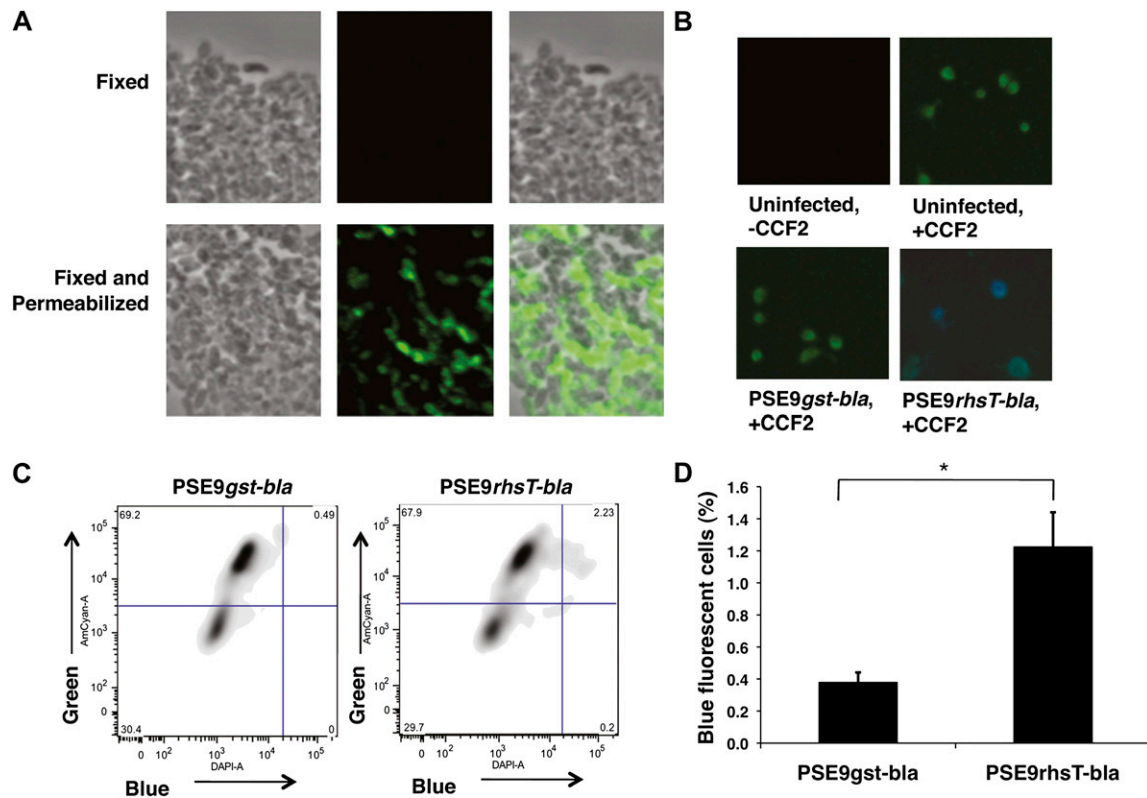


Fig. S2. RhsT localization and translocation studies. (A) Control experiments to demonstrate that the fixation process used in Fig. 2B did not permeabilize bacteria. PSE9 Δ rhsT(pRHST) bacteria were either fixed (*Upper*) or both fixed and permeabilized (*Lower*) as described in *Materials and Methods*. Immunofluorescence microscopy with an antibody against RNAP β , a cytosolic protein, revealed staining specific to bacteria that had been both fixed and permeabilized. The first column shows phase images, the second column shows immunofluorescence images, and the third column shows merged images. Magnification identical to Fig. 1B. (B) RhsT translocation into J774 murine macrophages in vitro. Microscopy was performed on J774 cells treated with CCF2-AM and infected with bacteria expressing RhsT- β -lactamase fusion protein. Cells were then visualized by fluorescence microscopy. Magnification, 40 \times . (C and D) RhsT translocation in vivo. At 15 h postinfection, cells were collected from the airways of mice infected with PSE9gst-bla or PSE9rhsT-bla and loaded with CCF2-AM. (C) Representative flow cytometry plots of recovered lung cells. The percentage of blue fluorescent cells is indicated in the upper right quadrant. The relatively small percentage of cells containing translocated RhsT- β -lactamase is likely because of death of cells following RhsT- β -lactamase translocation and removal from the viable cell pool. (D) Comparison of the percentage of blue fluorescent cells in the lungs of mice infected with PSE9gst-bla or PSE9rhsT-bla. Over two independent experiments, a total of five mice each were infected with PSE9gst-bla or PSE9rhsT-bla. In each experiment, bronchoalveolar lavage (BAL) fluid was collected and pooled for mice infected with the same strain at 15 h postinfection. Cells were collected from pooled BAL fluid and stained in triplicate with CCF2-AM. Percentage of blue fluorescent cells was determined using the same gating scheme shown in C. Data shown are mean percent blue cells \pm SEM ($n = 6$). * $P < 0.05$, two-tailed paired Student t test.

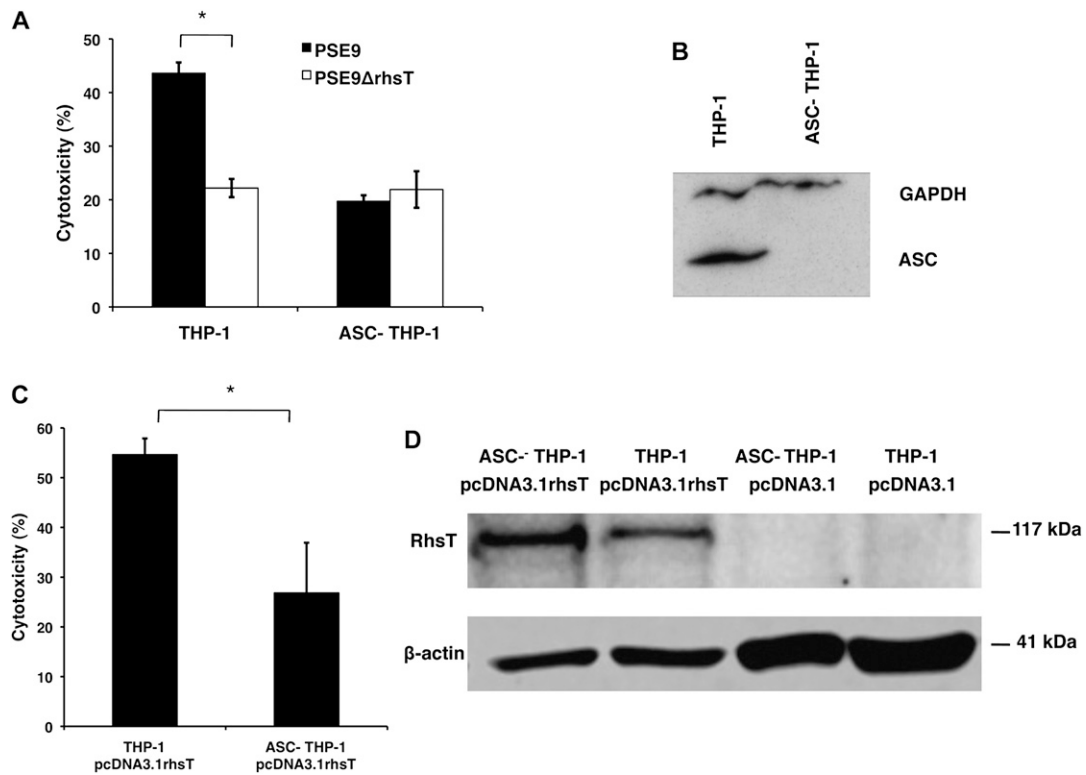


Fig. S3. RhsT-dependent cytotoxicity in the contexts of infection and transfection. (A) Infection of THP-1 cells with RhsT⁺ bacteria resulted in ASC-dependent cytotoxicity. Wild-type and ASC⁻ THP-1 cells were infected with bacteria at an MOI of 20, and lactate dehydrogenase (LDH) release into the medium was quantified at 4 h postinfection. **P* < 0.05, two-tailed paired Student *t* test. (B) Immunoblot analysis of ASC⁻ THP-1 cells verified the absence of detectable levels of ASC. Cell lysates were subjected to SDS/PAGE and protein transfer. Membrane was simultaneously probed with antibody to ASC (custom raised polyclonal using a peptide covering amino acids 93 through 111) and the loading control GAPDH (Santa Cruz). (C) RhsT is sufficient to cause ASC-dependent cell death. Wild-type and ASC⁻ THP-1 cells were transfected with empty vector (pcDNA3.1D/V5-His-TOPO, abbreviated pcDNA3.1) or an *rhsT*-expressing construct (pcDNA3.1*rhsT*). At 24 h posttransfection, cells were changed to fresh, serum-free medium, and 5 h later LDH release was quantified. Background LDH release from cells transfected with pcDNA3.1 was subtracted as described in *Materials and Methods*. Data are means ± SEM (*n* = 3). **P* < 0.05, two-tailed paired Student *t* test. (D) Immunoblot analysis verified RhsT expression in transfected THP-1 and ASC⁻ THP-1 cells. After supernatants were collected for analysis of cytotoxicity, the remaining cells were collected, lysed, and subjected to SDS/PAGE and protein transfer. Membrane was probed with an antibody to the V5 epitope (Invitrogen), which was added as a C-terminal tag to RhsT through cloning of *rhsT* into pcDNA3.1D/V5-His-TOPO (Invitrogen). The membrane was then stripped and rereprobed with an antibody to β-actin (Abcam). A band, presumably corresponding to an RhsT breakdown product, was detected near the 117-kDa molecular weight marker.

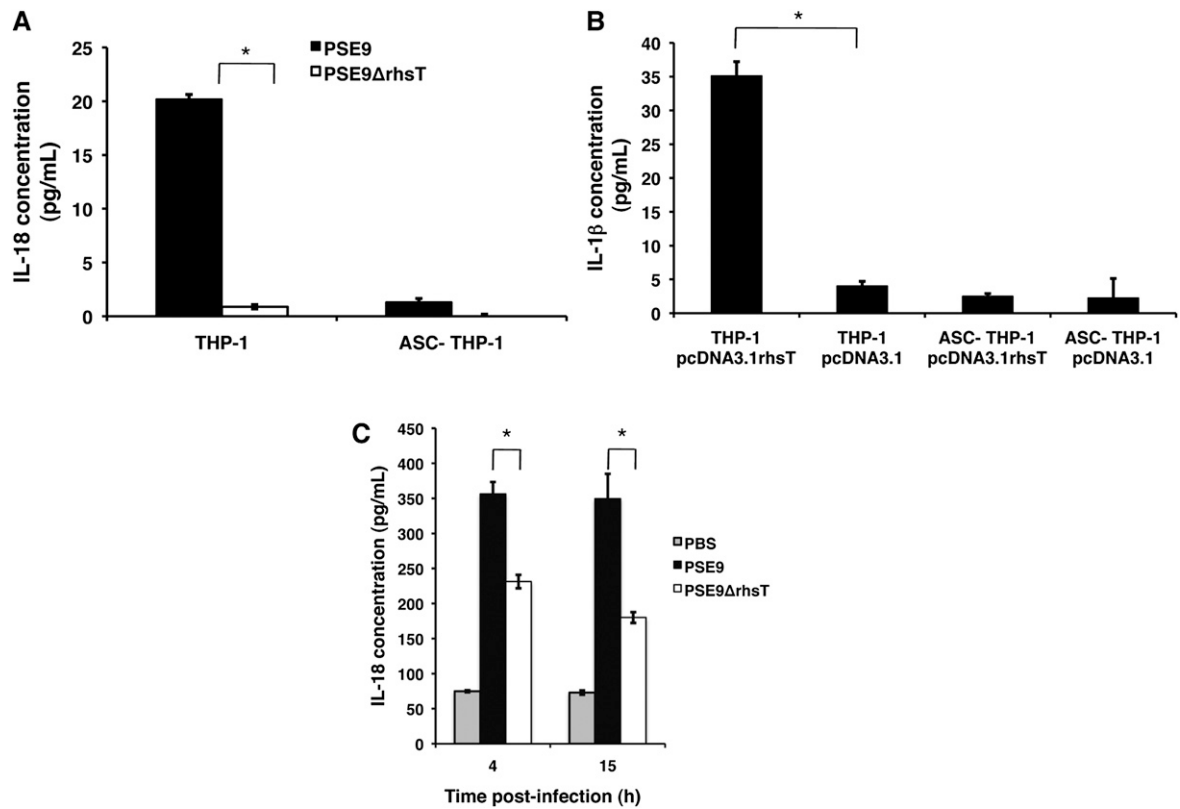


Fig. 54. RhsT-dependent IL-1 β and IL-18 release in the contexts of infection and transfection. (A) IL-18 release following infection of THP-1 cells in vitro. THP-1 and ASC⁻ THP-1 cells were infected at an MOI of 15 with PSE9 or PSE9 Δ *rhsT*. IL-18 levels were measured by ELISA at 3 h postinfection. (B) IL-1 β release following transfection of THP-1 cells. Wild-type and ASC⁻ THP-1 cells were transfected with empty vector (pcDNA3.1D/V5-His-TOPO, abbreviated pcDNA3.1) or an *rhsT*-expressing construct (pcDNA3.1*rhsT*). At 24 h posttransfection, cells were changed to fresh, serum-free medium, and 5 h later IL-1 β release was quantified by ELISA. Expression of RhsT was verified as described in Fig. S3D. (C) IL-18 release following infection in a mouse model of acute pneumonia. IL-18 levels in lung homogenates from mice infected with PSE9, PSE9 Δ *rhsT*, or PBS (mock infected) were determined by ELISA. Data are means \pm SEM ($n = 3$). * $P < 0.05$, two-tailed paired Student t test.

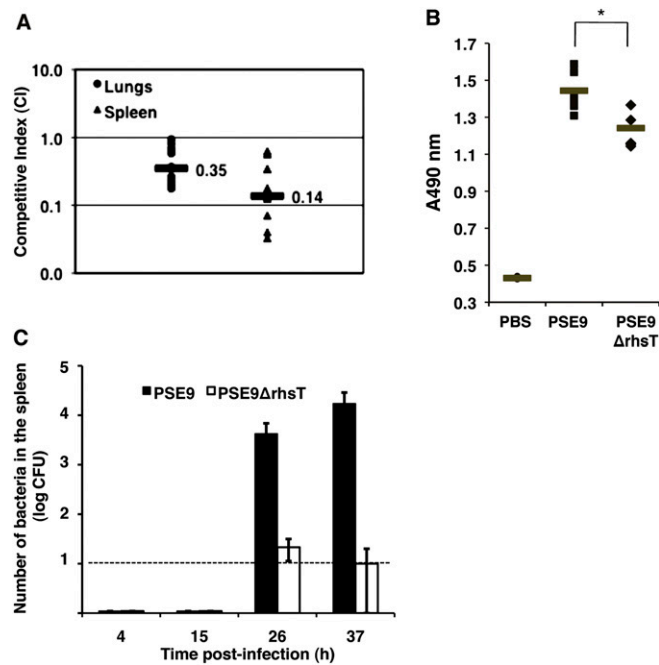


Fig. S6. Studies of RhsT virulence in a mouse model of acute pneumonia. (A) Competition assays between PSE9 and PSE9 Δ *rhsT* in the lungs of mice with acute pneumonia. Mice were coinfecting with 1.5×10^5 CFU each of PSE9 and PSE9 Δ *rhsT*. At 26 h postinfection, mice were killed and the CFU of mutant and parental bacteria present in the lungs and spleen were used to calculate a competitive index (CI). A CI < 1.0 indicates that the *rhsT* mutant is at a competitive disadvantage relative to the parental strain. Each symbol reflects the CI obtained for one mouse; bars indicate medians. (B) Role of RhsT in airway cell lysis. Mice were infected with 3.0×10^5 CFU of either PSE9 or PSE9 Δ *rhsT*. LDH levels were measured in BAL fluid collected at 26 h postinfection with PSE9, PSE9 Δ *rhsT*, or PBS using a colorimetric assay read at $A_{490\text{nm}}$. A higher $A_{490\text{nm}}$ value indicates more LDH release. Each symbol represents the value obtained for a single mouse; bars indicate medians ($n = 5$ for each group). * $P < 0.05$, two-tailed paired Student *t* test. (C) Role of RhsT in bacterial dissemination. Mice were infected with 3.0×10^5 CFU of either PSE9 or PSE9 Δ *rhsT* and killed at the indicated time points to determine the CFU in the spleen (limit of detection indicated by dotted line). Data shown are means \pm SEM ($n = 6$ for each time point). At 26 h postinfection, PSE9 dissemination was significantly greater than that of PSE9 Δ *rhsT* ($P < 0.001$, two-tailed paired Student *t* test).

Table S1. Description of strains used in this study

Strain	Description	Reference
PSE9	<i>P. aeruginosa</i> strain previously isolated from the BAL fluid of a patient who met strict criteria for ventilator-associated pneumonia.	(1)
PSE9 Δ <i>rhsT</i>	A strain where bp 309 through 6,124 of the 6,672-bp <i>rhsT</i> gene is replaced with a gentamicin resistance cassette.	Present study
PSE9 Δ <i>rhsT</i> +RHST	PSE9 Δ <i>rhsT</i> complemented with a wild-type <i>rhsT</i> allele under control of its native promoter at a neutral chromosomal site.	Present study
PSE9 Δ <i>rhsT</i> (pRHST)	PSE9 Δ <i>rhsT</i> complemented with <i>rhsT</i> on an arabinose inducible plasmid.	Present study
PSE9 Δ <i>rhsT</i> (pHERD)	PSE9 Δ <i>rhsT</i> containing an empty arabinose inducible plasmid.	Present study
PSE9 <i>rhsT-bla</i>	PSE9 containing <i>rhsT-bla</i> under control of the native <i>rhsT</i> promoter at a neutral chromosomal site.	Present study
PSE9 <i>gst-bla</i>	PSE9 containing <i>gst-bla</i> under control of the native <i>rhsT</i> promoter at a neutral chromosomal site.	Present study
M90T	Invasive <i>Shigella flexneri</i> strain previously shown to activate caspase-1.	(2)
BS176	<i>S. flexneri</i> strain derived from M90T by curing it of its type III secretion virulence plasmid.	(3)

- Hauser AR, et al. (2002) Type III protein secretion is associated with poor clinical outcomes in patients with ventilator-associated pneumonia caused by *Pseudomonas aeruginosa*. *Crit Care Med* 30:521–528.
- Hilbi H, et al. (1998) *Shigella*-induced apoptosis is dependent on caspase-1 which binds to IpaB. *J Biol Chem* 273:32895–32900.
- Zychlinsky A, Prevost MC, Sansonetti PJ (1992) *Shigella flexneri* induces apoptosis in infected macrophages. *Nature* 358:167–169.

Table S2. Primer sequences

Primer	Sequence
rhsT-5'-F-NgoMIV	AAA AAA GCC GGC AAA ATT CGA TGA GGG CCC GC
rhsT -5'-R-Xmal	AAA AAA CCC GGG AAT CGT TCG GCT GCA GGA TC
rhsT -3'-F-Xmal	AAA AAA CCC GGG CTG GTT TTG GGG AAT GCC TT
rhsT -3'-R-NgoMIV	AAA AAA GCC GGC AAT TCC TCC AGT AGT GCC CAC
rhsT -F-SpeI	AAA AAA ACT AGT CGA TCT CCT GAT TGT ATT GGC
rhsT -R-Xmal	AAA AAA CCC GGG TCA CAT CCC TCT CCG GTG CTC
rhsT -F-Xba1	AAA AAA TCT AGA CAA CCA AAG ATA TGT GGC
rhsT -R-Nsil	AAA AAA ATG CAT CAA TTG GCC ACA TAT
gst-F-Nsil	AAA AAA ATG CAT ATG TCC CCT ATA CTA GGT TAT
rhsT -R-Δstop-Xmal	AAA AAA CCC GGG CAT CCC TCT CCG GTG CTC
bla-F-Xmal	AAA AAA CCC GGG CAC CCA GAA ACG CTG GTG A
bla-R-Xmal	AAA AAA CCC GGG TTA CCA ATG CTT AAT CAG TGA
bla-R-Nsil	AAA AAA ATG CAT TTA CCA ATG CTT AAT CAG TGA
rhsT -qPCR-F	CATCTTTCAAGTGGCTCGCCC
rhsT -qPCR-R	GTAGGCCAAGCGCTCGACAT
oprL-qPCR-F	GCGTGGATCACACCTTCT
oprL-qPCR-R	TATTGTACTCGCGGGTCCG
GSP1	GGA ATC GTT CCG CTG CAG G
GSP2	CAG GTC GAG GAT GCC ATG GCG ATT
GSP3	CTG GTC GCC GAT GAA GCT CTG GAT GG
pcDNA3.1rhsT-F	CAC CAT GGT CCG GGA CGC GAC CGC
pcDNA3.1rhsT-R	CAT CCC TCT CCG GTG CTC AAC

Table S3. Description of plasmids used in this study

Plasmid	Description
pEX100TrhsT	Used to generate strain PSE9Δ <i>rhsT</i> . An ~500-bp DNA fragment extending from upstream to within the 5' coding region of <i>rhsT</i> was amplified by PCR using the NgoMIV and Xma1 restriction-enzyme-compatible primers rhsT -5'-F-NgoMIV and rhsT -5'-R-Xmal. The same approach was used with primers rhsT-3'-F and rhsT -3'-R to amplify an ~500-bp DNA fragment overlapping the 3' portion of the <i>rhsT</i> gene. The amplified DNA fragments were digested with NgoMIV and Xma1, gel purified, and then sequentially ligated and cloned into the Xma1 site of pEX100T (1). A 2.3-kb gentamicin resistance cassette generated by Xma1 digestion of pX1918G (1) was then cloned into the Xma1 site between the two fragments.
mini-CTX1 <i>rhsT</i>	Used to generate strain PSE9Δ <i>rhsT</i> +RHST. The <i>rhsT</i> allele along with 412 bp upstream were amplified by PCR using primers rhsT-F-SpeI and rhsT -R-Xmal, gel-purified, digested with SpeI and Xma1, and ligated into plasmid mini-CTX1 (2).
mini-CTX1 <i>rhsT</i> - <i>bla</i>	Used to generate strain PSE9 <i>rhsT</i> - <i>bla</i> . The <i>rhsT</i> allele along with 412 bp upstream was amplified using primers rhsT-F-SpeI and rhsT-R-Δstop-Xmal and was cloned into plasmid mini-CTX1. The gene encoding TEM-1 Bla was then amplified from plasmid pBR322 using primers bla-F-Xma1 and bla-R-Xma1 and cloned into the modified mini-CTX1 vector.
mini-CTX1 <i>gst</i> - <i>bla</i>	Used to generate strain PSE9 <i>gst</i> - <i>bla</i> . A 412-bp DNA fragment upstream of the <i>rhsT</i> allele was amplified using primers rhsT-F-SpeI and rhsT-R-Nsil and cloned into plasmid mini-CTX1. Subsequently, the <i>gst</i> - <i>bla</i> gene was amplified from mini-CTX <i>gst</i> - <i>bla</i> (3) using primers gst-F-Nsil and bla-R-Nsil and ligated into the modified mini-CTX1 vector.
pRHST	Used to generate strain PSE9Δ <i>rhsT</i> (pRHST). The <i>rhsT</i> gene was amplified by PCR using primers rhsT-F-Xba1 and rhsT-R-Xmal, gel-purified, digested with Xba1 and Xma1, and ligated into plasmid pHERD20T.
pHERD20T	A P _{BAD} -based arabinose inducible expression plasmid (4).

- Schweizer HP, Hoang TT (1995) An improved system for gene replacement and xylE fusion analysis in *Pseudomonas aeruginosa*. *Gene* 158:15–22.
- Hoang TT, Kutchna AJ, Becher A, Schweizer HP (2000) Integration-proficient plasmids for *Pseudomonas aeruginosa*: Site-specific integration and use for engineering of reporter and expression strains. *Plasmid* 43:59–72.
- Diaz MH, Hauser AR (2010) *Pseudomonas aeruginosa* cytotoxin ExoU is injected into phagocytic cells during acute pneumonia. *Infect Immun* 78:1447–1456.
- Qiu D, Damron FH, Mima T, Schweizer HP, Yu HD (2008) PBAD-based shuttle vectors for functional analysis of toxic and highly regulated genes in *Pseudomonas* and *Burkholderia* spp. and other bacteria. *Appl Environ Microbiol* 74:7422–7426.